On-Column Micro Gas Chromatography Detection with Capillary-Based Optical Ring Resonators

Siyka I. Shopova,[†] Ian M. White,[†] Yuze Sun,[†] Hongying Zhu,[†] Xudong Fan,*,[†] Greg Frye-Mason,[‡] Aaron Thompson,[§] and Shiou-jyh Ja[§]

Biological Engineering Department, University of Missouri-Columbia 240D Bond Life Sciences Center, 1201 East Rollins Street, Columbia, Missouri 65211, ICx Nomadics, 1001 Menaul Blvd North East, Suite A, Albuquerque, New Mexico 87107, and ICx Nomadics, 1024 South Innovation Way, Stillwater, Oklahoma 74074

We developed a novel on-column micro gas chromatography (μGC) detector using capillary based optical ring resonators (CBORRs). The CBORR is a thin-walled fused silica capillary with an inner diameter ranging from a few tens to a few hundreds of micrometers. The interior surface of the CBORR is coated with a layer of stationary phase for gas separation. The circular cross section of the CBORR forms a ring resonator and supports whispering gallery modes (WGMs) that circulate along the ring resonator circumference hundreds of times. The evanescent field extends into the core and is sensitive to the refractive index change induced by the interaction between the gas sample and the stationary phase. The WGM can be excited and monitored at any location along the CBORR by placing a tapered optical fiber against the CBORR, thus enabling on-column real-time detection. Rapid separation of both polar and nonpolar samples was demonstrated with subsecond detection speed. Theoretical work was also established to explain the CBORR detection mechanism. While low-nanogram detection limits are observed in these preliminary tests, many methods for improvements are under investigation. The CBORR is directly compatible with traditional capillary GC columns without any dead volumes. Therefore, the CBORR-based μGC is a very promising technology platform for rapid, sensitive, and portable analytical devices.

Increasing environmental and safety concerns are driving the development of small, highly sensitive, and selective gas sensors. However, most gas sensors respond to a group of chemicals and lack sensing selectivity, which significantly hinders their utility. In contrast, in gas chromatography (GC), gaseous samples are separated based on their interaction with the stationary phase coated on a GC channel and, therefore, can be separated and identified by their respective retention time in the channel. One major drawback with the conventional GC is that the required equipment is large, power intensive, and requires long analysis times. Research on μGC analyzers over the past 10 years has

shown great potential for small, rapid, and low-power μGC systems.[1–10] However, in those μGC systems, the gas detection is typically carried out at the terminal end of the GC channel, which requires complicated fluidic connection, leading to decreased reliability and dead volumes that degrade separation and decrease detection speed and sensitivity. Additionally, most μGC systems rely on rectangular microfabricated GC channels. While significant progress in high-efficiency separations using rectangular GC columns has been reported recently based on tailored etching and coating techniques,[3,8–10] our circular GC channels will not suffer from nonuniformities in stationary phase coating at corners or at fluidic connections to the etched columns, which can be a cause of degraded separation performance.[2,4,8] On-column detection performed on a circular GC capillary is highly desirable to simplify the fluidic design and to achieve high resolution in GC detection.

In this paper, we demonstrate sensitive and rapid μGC detection using a capillary based optical ring resonator (CBORR), as illustrated in Figure 1A. The CBORR is an emerging photonic sensing technology recently developed in one of our labs.[11–13] As shown in Figure 1B, the CBORR employs a micro-sized glass capillary, whose inner surface is coated with a layer of polymer

* Corresponding author. E-mail: fanxud@missouri.edu. Phone: 573-884-2543. Fax: 573-884-9676.
† University of Missouri-Columbia.
‡ ICx Nomadics, Albuquerque, New Mexico.
§ ICx Nomadics, Stillwater, Oklahoma.

(1) Cai, Q. Y.; Zellers, E. T. *Anal. Chem.* **2002**, *74*, 3533–3539.
(2) Frye-Mason, G.; Kottenstette, R.; Mowry, C.; Morgan, C.; Manginell, R.; Lewis, P.; Matzke, C.; Dulleck, G.; Anderson, L.; Adkins, D. In *Proceeding of Micro Total Analysis Systems Workshop*; Ramsey, J. M., Van Den Berg, A. J., Eds.; 2001; pp 658–660.
(3) Lambertus, G.; Sacks, R. *Anal. Chem.* **2005**, *77*, 2078–2084.
(4) Lewis, P. R.; Manginell, R. P.; Adkins, D. R.; Kottenstette, R. J.; Wheeler, D. R.; Sokolowski, S. S.; Trudell, D. E.; Byrnes, J. E.; Okandan, M.; Bauer, J. M.; Manley, R. G.; Frye-Mason, G. C. *IEEE Sensors J.* **2006**, *6*, 784–795.
(5) Lu, C.-J.; Steinecker, W. H.; Tian, W.-C.; Oborny, M. C.; Nichols, J. M.; Agah, M.; Potkay, J. A.; Chan, H. K. L.; Driscoll, J.; Sacks, R. D.; Wise, K. D.; Pang, S. W.; Zellers, E. T. *Lab Chip* **2005**, *5*, 1123–1131.
(6) Noh, H.; Hesketh, P. J.; Frye-Mason, G. C. *J. Microelectromech. Syst.* **2002**, *11*, 718–725.
(7) Stadermann, M.; McBrady, A. D.; Dick, B.; Reid, V. R.; Noy, A.; Synovec, R. E.; Bakajin, O. *Anal. Chem.* **2006**, *78*, 5639–5644.
(8) Lambertus, G.; Elstro, A.; Sensenig, K.; Potkay, J.; Agah, M.; Scheuering, S.; Wise, K.; Dorman, F.; Sacks, R. *Anal. Chem.* **2004**, *76*, 2629–2637.
(9) Reidy, S.; George, D.; Agah, M.; Sacks, R. *Anal. Chem.* **2007**, *79*, 2911–2917.
(10) Reidy, S.; Lambertus, G.; Reece, J.; Sacks, R. *Anal. Chem.* **2006**, *78*, 2623–2630.
(11) White, I. M.; Oveys, H.; Fan, X. *Opt. Lett.* **2006**, *31*, 1319–1321.
(12) White, I. M.; Oveys, H.; Fan, X.; Smith, T. L.; Zhang, J. *Appl. Phys. Lett.* **2006**, *89*, 191106.
(13) White, I. M.; Suter, J. D.; Oveys, H.; Fan, X.; Smith, T. L.; Zhang, J.; Koch, B. J.; Haase, M. A. *Opt. Express* **2007**, *15*, 646–651.
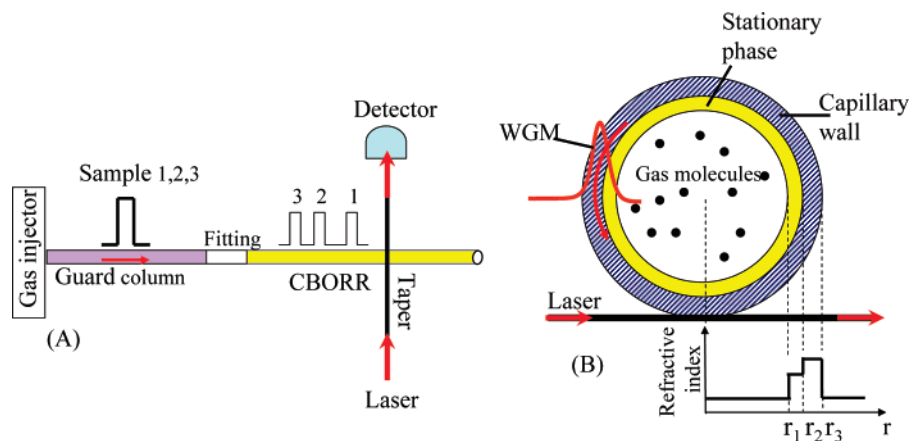
Figure 1. Concept and experimental setup for CBORR-based GC. (A) The sample is introduced in the gas injector, after which it travels as a short pulse carried by high purity hydrogen gas. The chemically inert guard column is connected to the Carbowax coated CBORR by a press tight fitting. The separation of different compounds in the sample is enabled by their different interaction with the stationary phase. Optical detection is performed by measuring the transmission through a tapered optical fiber in contact with the CBORR. (B) Cross section of the CBORR showing the propagation of a WGM confined in the coated capillary wall. r_1, inner radius; r_2, radius at the polymer coating layer, and r_3, outer radius. Dimensions are not to scale.

as a stationary phase, to conduct the gaseous samples. The circular cross section of the capillary forms a ring resonator that supports whispering gallery modes (WGMs).[14,15] A waveguide, such as an optical fiber taper arranged perpendicular to the capillary, couples resonant light into the WGM, thus defining an interrogation location along the capillary. This narrow detection zone allows for decreasing the length of the coated column, which leads to very fast detection times. The capillary wall is sufficiently thin (<4 μm) so that the evanescent field of the WGM is exposed to the core.

Refractive index (RI) changes near the CBORR interior surface induced by the absorption of the gas samples into the polymer can be detected in real time by monitoring the WGM spectral position, which is governed by

$$\lambda = \frac{2\pi n_{\text{eff}} r}{l} \tag{1}$$

where λ is the resonant wavelength, r is the ring radius, n_{eff} is the effective RI experienced by the WGM, and l is an integer that represents the angular momentum of the WGM. Therefore, the WGM spectral shift in response to sample interaction with the polymer in the CBORR provides both quantitative and kinetic information about the movement of the gas samples in the capillary. Furthermore, the ring resonator design leads to high sensitivity with a small detection area because the circulating mode repeatedly interacts with the sample. The effective interaction length, L_{eff}, is related to the optical quality factor (Q) by[14,15] $L_{\text{eff}} = Q\lambda/2\pi n_{\text{eff}}$. For a ring resonator with a Q-factor of 10^6, $n_{\text{eff}} = 1.45$, and $\lambda = 1550$ nm, L_{eff} can be as long as 17 cm, despite the small physical size of a resonator (50–200 μm in diameter).

The circular capillary sensor is also highly compatible as a detection mechanism with GC technologies. Well-established column-coating techniques can be used without any significant modifications to provide uniform stationary phase coatings. In addition, analyte separation and detection are carried out in situ within the same column. This unique on-column analysis can be conducted at any location along the column, which is not feasible with conventional GC detectors that are separated from the GC column. Furthermore, the CBORR can be coated with different polar and nonpolar stationary phase to increase the GC separation capability and to increase the sensitivity and selectivity for detection of particular classes of analytes.

DETECTION THEORY

The WGM of a CBORR can be fully described using the Mie theory by considering a three-layered radial structure (core, wall, and surrounding medium), as presented previously.[11,16,17] In the case of the CBORR for μGC, a four-layer model that includes the polymer layer on the inner CBORR surface is necessary, as illustrated in Figure 1B. The radial distribution of the WGM electrical field of a CBORR is governed by

$$E_{m,l}(r) = \begin{cases} AJ_m(k_{m,l}n_1 r) & (r \le r_1) \\ BJ_m(k_{m,l}n_2 r) + CH_m^{(1)}(k_{m,l}n_2 r) & (r_1 \le r \le r_2) \\ DJ_m(k_{m,l}n_3 r) + EH_m^{(1)}(k_{m,l}n_3 r) & (r_2 \le r \le r_3) \\ FH_m^{(1)}(k_{m,l}n_4 r) & (r \ge r_3) \end{cases} \tag{2}$$

where J_m and $H_m^{(1)}$ are the mth Bessel function and the mth Hankel function of the first kind, respectively. n_1, n_2, n_3, and n_4 are the RI of the core, the polymer layer, the resonator wall, and the surrounding medium, respectively. r_1, r_2, and r_3 designate the radius at the inner surface, at the resonator wall, and at the outer surface, as shown in Figure 1B. The resonant wavelength and corresponding radial field intensity can be calculated by matching the boundary conditions at r_1, r_2, and r_3. The calculated radial mode

(14) Chang, R. K.; Campillo, A. J. *Optical Processes in Microcavities*; World Scientific: Singapore, 1996.

(15) Gorodetsky, M. L.; Savchenkov, A. A.; Ilchenko, V. S. *Opt. Lett.* **1996**, *21*, 453–455.

(16) Bohren, C. F.; Huffman, D. R. *Absorption and Scattering of Light by Small Particles*; John Wiley & Sons: New York, 1998.

(17) Fan, X.; White, I. M.; Zhu, H.; Suter, J. D.; Oveys, H. In *SPIE Laser Resonators and Beam Control X*; Kudryashov, A. V., Paxton, A. H., Ilchenko, V. S., Eds.; 2007; Vol. 6452, p 64520M.
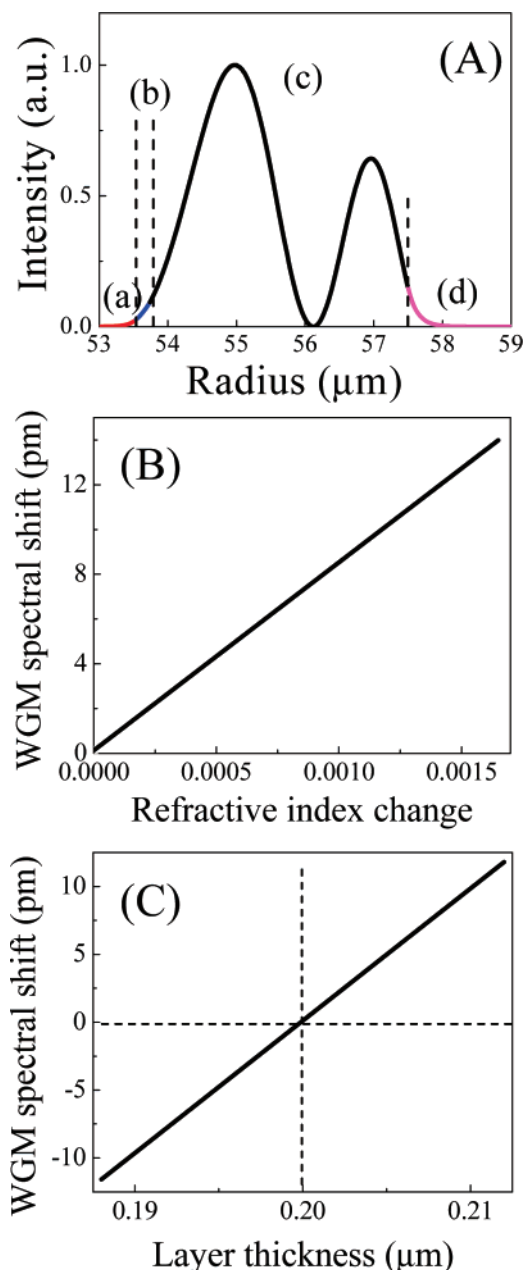
Figure 2. (A) Calculated WGM intensity distribution for a CBORR with 115 μm o.d., 3.96 μm wall thickness, and 200 nm thick polymer coating thickness. The refractive indices are 1.0, 1.465, 1.45, and 1.0 for (a) core, (b) polymer coating, (c) capillary wall, and (d) the surrounding medium, respectively. (B) The WGM spectral shift of this mode as a function of the change in the refractive index of the polymer layer. (C) The WGM spectral shift of this mode as a function of change in the thickness of the polymer layer. Two narrow-spaced dashed lines on the left are for 200 nm thick polymer layer. The dashed line on the right indicates the CBORR outer surface.

intensity of the second-order radial mode for the CBORR used in our experiment is plotted in Figure 2. The WGM field extends through the polymer layer. As the gas molecules absorb into the stationary phase, the RI of the layer or its thickness will change, resulting in a modification in the effective RI (n_{eff}), which in turn causes the WGM spectral position to shift. Although changes in the polymer RI and thickness may occur concomitantly for each gas sensing, we separately plot these two effects on the WGM spectral shift in parts B and C of Figure 2. Note that the WGM

spectral shift can be negative with respect to the baseline obtained in the absence of the gas sample, if the RI of the polymer layer decreases or the polymer shrinks upon interaction with the gas sample, as shown in parts B and C of Figure 2. This is in contrast to conventional GC detectors, in which only positive signals are generated.

EXPERIMENTAL SECTION

In our experiment, a 10 cm long CBORR (115 μm outer diameter (o.d.)) was fabricated by rapidly stretching a preform (TSP530660 from Polymicro, o.d. = 616 μm and wall thickness = 40 μm, or Q120-90-7.5 from Sutter Instrument, o.d. = 1200 μm and wall thickness = 150 μm) under heat, followed by HF etching to further reduce the wall thickness. The CBORR wall thickness was determined from the measured RI sensitivity of the WGM. The CBORR fabrication and wall thickness characterization was described in detail in ref 11. The wall thickness of the CBORR was estimated to be 4 μm. Then the CBORR was coated with Carbowax 400 (Supelco, n = 1.465), a polar polymer that acts as the stationary phase. We employed the static coating method.[10] To achieve this, the CBORR was initially filled with 7.5 mg/mL Carbowax in acetone for 1 h, followed by acetone evaporation under vacuum. The thickness of the Carbowax layer was estimated to be approximately 200 nm. The Q-factor of the CBORR is over 10^6, corresponding to a WGM line width of approximately 1 pm.

Gas samples were extracted from the saturated vapor in the head space of the analyte sample vials with a solid-phase microextractor (SPME)[18] (PDMS/DVB, 65 μm diameter fiber, Supelco 57310-U) and introduced into a GC injection system (HP 5890, heated to 250 °C), which generated a gas pulse as illustrated in Figure 1A. The gas pulse traveled along a 1.8 m, 0.25 mm inner diameter (i.d.) nonpolar passivated fused silica guard column (Supelco), which had minimal interaction with the analyte. The guard column was connected with the CBORR via a universal quick seal column connector (Varian). Ultrahigh purity hydrogen gas (H$_2$ UHP300) was used as a carrier gas. As illustrated in Figure 1A, a tapered optical fiber was brought in contact with the CBORR at a location 6 cm away from the CBORR inlet. A 1550 nm tunable diode laser was coupled into the end of the optical fiber and was scanned in wavelength at a rate of 2−10 Hz. A detector (Figure 1A) was used to monitor the light intensity at the distal end of the fiber. Each time the laser scans through a wavelength that matches the resonant condition of a WGM in eq 1, the laser light is coupled to the resonator, leaving a spectral dip at the fiber output, which can be used to indicate the WGM spectral position.[11] As the gas pulse passed through the CBORR, it interacted with the coating layer, which led to a WGM spectral shift. A LabView program was used to control the data acquisition. The WGM spectral position was analyzed by a homemade program, which displayed the WGM spectral shift as a function of time (chromatogram). The CBORR optical response was also compared with the peak measured by a conventional flame-ionization detector (FID). Analyte mass collected on the SPME was calibrated using a Varian 3800 gas chromatograph with a Saturn 2000 ion trap mass spectrometer.

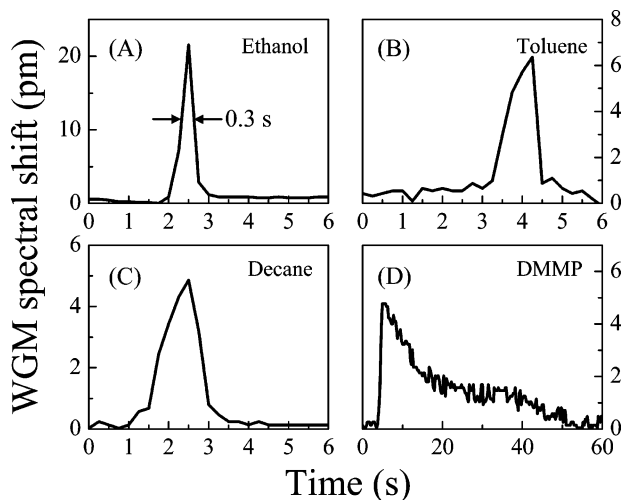(18) Zhang, Z.; Pawliszyn, J. *Anal. Chem.* **1993**, *65*, 1843−1852.

Figure 3. WGM shift upon injection of various analytes: (A) ethanol with a flow rate of 3.30 mL/min and split ratio 27:1; (B) toluene with a flow rate 3.30 mL/min and split ratio 27:1; (C) decane with a flow rate 6.8 mL/min and split ratio 50:1; (D) DMMP with a flow rate 9.6 mL/min and split ratio 50:1.

RESULTS AND DISCUSSION

Our initial work shows the potential of the CBORR for rapid on-column detection of different analytes with various volatilities and both polar and nonpolar analytes. Figure 3 shows the measured WGM shift for ethanol, toluene, decane, and dimethyl methylphosphonate (DMMP). Each scan was taken twice to ensure repeatability (only one chromatogram is shown). The selection of analytes covers nonpolar organic compounds such as highly volatile toluene and less volatile decane as well as slightly polar (ethanol) and highly polar (DMMP) organic compounds. As discussed previously, the shift of the WGM is proportional to the change of the effective RI in the polymer layer, which is affected by the presence of a fraction of analyte molecules in the stationary phase. Therefore, the WGM shift should reflect the interaction between the gas analyte and the stationary phase, which is determined by the mass absorbed in the stationary phase. For nonpolar and slightly polar analytes that do not interact strongly with the stationary phase, sharp peaks are measured, indicative of rapid absorption/desorption processes. Figure 3A shows a sharp peak associated with volatile ethanol. The peak width is smaller than 0.3 s, limited by our laser scanning rate (<10 Hz). Using a higher laser scanning rate, we should be able to resolve a much sharper peak. For DMMP, a very polar analyte, it interacts strongly with the stationary phase. As a result, DMMP has much longer retention time inside the CBORR, and as illustrated in Figure 3D, shows a slow return of the WGM spectral shift back to the baseline. This tailing effect was also observed in previous studies.[19]

Figure 4 shows a very interesting phenomenon that the WGM has a negative shift upon the injection of the polar chemical triethylphosphate (TEP). Although the detailed mechanism of this negative shift is still under investigation, we speculate that the interaction of TEP with the polymer layer causes the layer to shrink, which has a larger effect than the RI increase in the
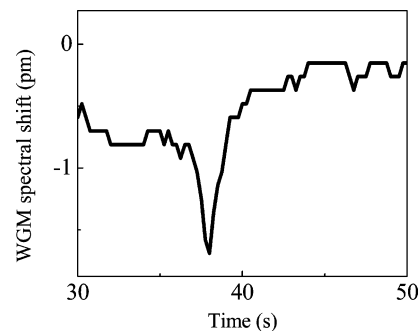

Figure 4. Negative WGM shift observed after injection of TEP. The flow rate was 5.7 mL/min and the split ratio was 45:1.

polymer layer, thus leading to an overall negative shift in the WGM spectral position. Note that in contrast to traditional GC detectors such as mass spectrometry and FID where the signal is always positive, this potential for both positive and negative signal in this optical detection system provides another mechanism for molecular identification.

In order to determine the CBORR's response to changes in the analyte mass, we increased the mass of the analyte injected in the capillary by increasing the SPME sampling time. In this experiment, we used decane with a flow rate of 6.8 mL/min and a GC injection split ratio of 50:1 ($^1/_{50}$th of the actual extraction goes to the gas column). The quantity of decane for each injection was later calibrated with GC/MS. The chromatogram for each injection is plotted in Figure 5A. Figure 5B shows the linear relationship between the area under the decane peak (WGM shift integrated over time) and the gas mass injected into the CBORR. Figure 5C plots the peak height with injected mass, showing a linear relationship up to about 200 ng injection levels. There is a leveling off at higher mass due to increasing peak width, which is likely a result of overloading the column, since the peak shape shows a tendency to have a slower rise consistent with overloading (Figure 5A). This overloading and peak broadening are not surprising, considering the large injection amounts used in this initial demonstration, especially since we were using a very short microbore column with only a passivated guard column between the injector and the CBORR. Improvements in noise levels enabling lower detection levels and in system design to improve separations will allow us to significantly increase the linear range for detection. We do not anticipate that the peak broadening observed in Figure 5A will be an issue for future applications since it occurs at injection amounts much larger than will be relevant for most applications. The detection limit of this GC detector can be estimated by the smallest resolvable WGM shift. In Figure 5, no temperature control was implemented. Therefore, the WGM spectral position is subject to temperature-induced fluctuation due to ambient air flow. In Figure 6, we used a simple passive control in which the CBORR was placed in a plastic enclosure. The noise level is approximately 0.15 pm (3σ). Using 0.15 pm, the detection limit for decane in Figure 5 is estimated to be 4.5 ng. Note that with an active temperature control, a noise level of 0.02 pm can be achieved,[20] leading to an even lower detection limit.

To demonstrate the separation capability of the CBORR based μGC, we simultaneously injected mixtures of various analytes. In

(19) Whiting, J. J.; Lu, C.-J.; Zellers, E. T.; Sacks, R. D. *Anal. Chem.* **2001**, *73*, 4668−4675.

(20) Zhu, H.; White, I. M.; Suter, J. D.; Zourob, M.; Fan, X. *Anal. Chem.* **2007**, *79*, 930−937.
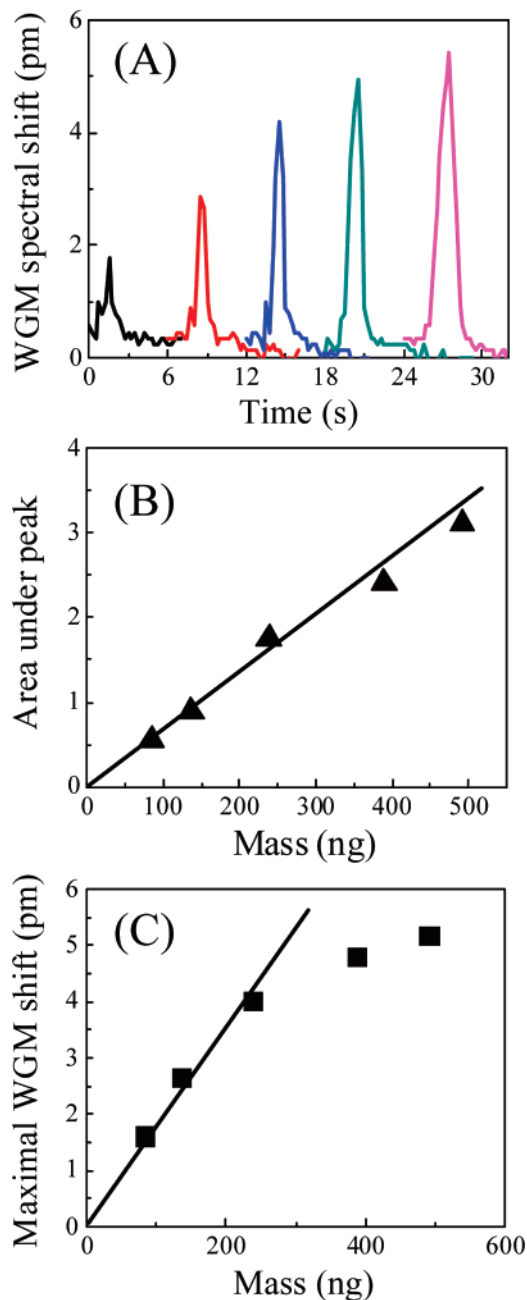
Figure 5. (A) WGM response to decane with various SPME exposure time. The chromatograms are horizontally shifted for clarity. (B) Linear dependence of the area under the peak versus amount of decane. Solid line is the linear fit. (C) The peak height as a function of mass. Solid line is the linear fit using the data below 200 ng.

conventional GC and μGC systems, separation occurs as the sample travels through a separation column that is several tens of meters long for conventional GC and is on the order of a meter or more for μGC. In this experiment, the distance between the CBORR inlet and the location where the optical taper was placed was only 1.5 cm. Figure 7 shows separation of ethanol/decane (Figure 7A), toluene/decane (Figure 7B), toluene/DMMP (Figure 7C), and decane/DMMP (Figure 7D). The ability to separate several different samples over a short distance is enabled by the small size of the detector.

The repeatability of gas sample separation is presented in Figure 8. The separation peaks of the mixed gaseous analytes
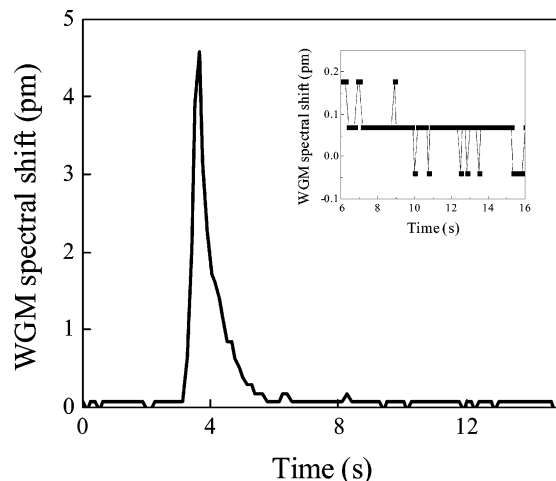
Figure 6. Chromatogram for toluene when the passive temperature control was implemented. Inset: a magnified view of the baseline noise. $\sigma = 0.05$ pm.
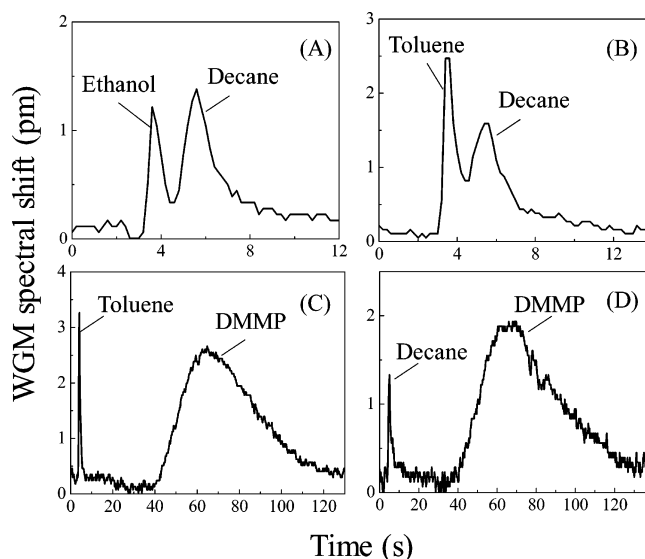

Figure 7. Separation of different analytes after passing through the 1.5 cm of Carbowax coated CBORR. SPME extraction time: ethanol, $\sim$8 s; decane, $\sim$10 s; toluene, $\sim$5 s; and DMMP, $\sim$10 s.

match those for each individual analyte quite well, irrespective of the analyte concentration (peak height) (Figure 8A,B). Although manual sample injection may introduce a certain degree of variation in retention time measurement, using a gas marker can significantly improve such measurement, as demonstrated in Figure 8C, in which decane was used as a marker.

Since the WGM measures the stationary phase (or polymer layer) change when it interacts with the gas analyte flowing in the capillary, it is critical to verify whether the detection signal generated by the WGM reflects the flow profile in the capillary. Here we used DMMP as a model system and a CBORR in which the distance between the CBORR inlet and the optical taper is approximately 1 cm. Reducing the length to 1 cm significantly reduces the retention time of the highly polar DMMP sample, resulting in a much sharper peak than that in Figure 3D where the length was 6 cm. In Figure 9, we compare the FID response (Figure 9A) and the WGM spectral shift in the CBORR (Figure 9B) after an SPME injection of DMMP sample. The FID measurement was carried out separately at the inlet of the CBORR (or
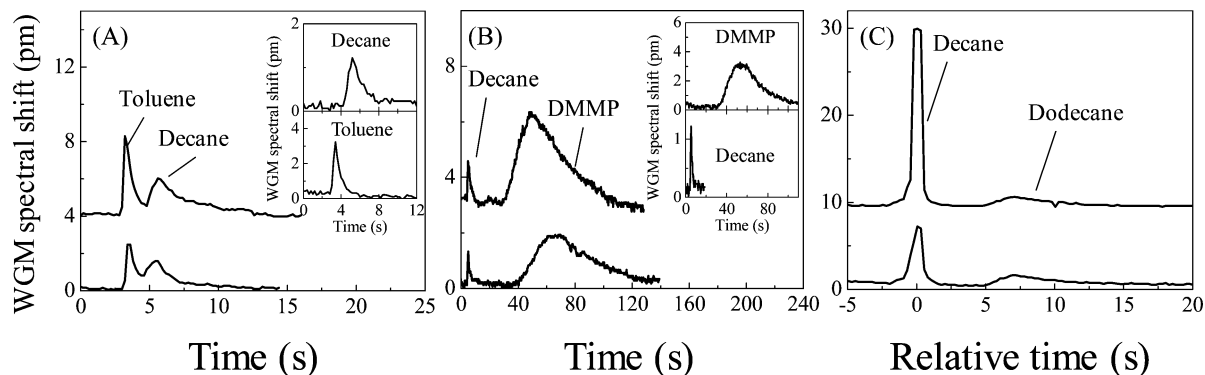
Figure 8. Chromatogram repeatability test: (A) separation between toluene and decane; (B) separation between decane and DMMP; (C) relative separation between decane and dodecane. The insets in parts A and B are the chromatogram for each individual gas component. Variation in peak height was due to the variations in SPME sampling time. Curves are shifted vertically for clarity.
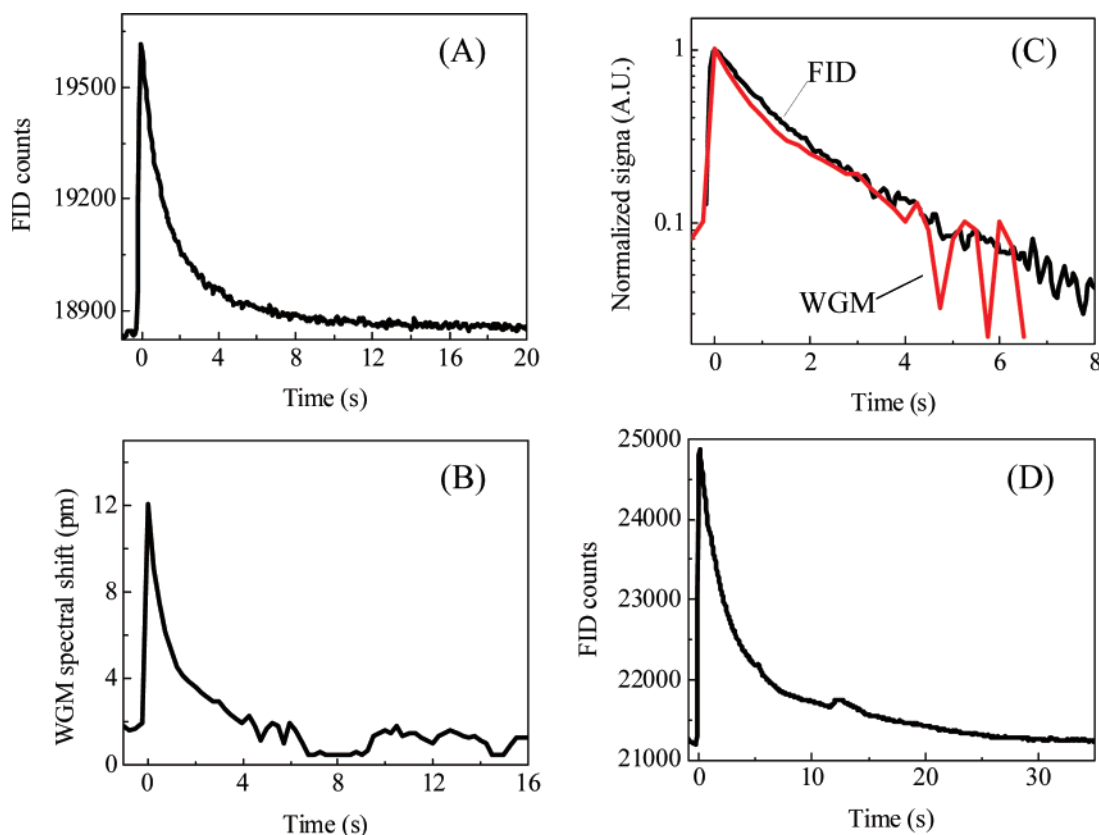

Figure 9. Comparison between the CBORR detection and conventional FID detection. (A) FID chromatogram of DMMP right after the 1 m guard column and before the CBORR inlet. (B) CBORR chromatogram of DMMP. (C) Overlay of normalized FID and WGM signal in logarithm scale. The flow rate was 7.2 mL/min and the split ratio 50:1. Note that two independent data acquisition systems were employed for the respective CBORR and FID measurement. (D) FID chromatogram after the 1 m guard column, CBORR, and another 1 m guard column.

outlet of the guard column). The two chromatograms have very similar shape and comparable time response, suggesting that the CBORR measurement does reflect the sample flow profile in a column. The calibration using liquid injection indicated that 47 ng of DMMP was used in Figure 9B. Assuming the 0.15 pm detection limit discussed early, the CBORR is capable of detecting 0.6 ng of DMMP. Figure 9D plots the chromatograms measured after the CBORR, which obviously becomes much broader than in Figure 9A, highlighting the fact that DMMP interacted more with the Carbowax in the CBORR.

DISCUSSION

While the initial demonstration of this unique on-column detector shows promise, it also highlights that there are many

ways to optimize the performance of this technology. For example, longer capillaries that have longer retention time are suitable for more volatile analytes, while highly polar and less volatile analytes, such as DMMP, require significantly shorter actively coated capillaries. Furthermore, the separation and detection capabilities can be tailored by applying different coatings on the inner CBORR surface and by coupling the CBORR with conventional GC columns. The CBORR sensitivity can also be enhanced by optimizing the stationary phase deposition, including polymer thickness and uniformity, to achieve better light−analyte interaction. The CBORR wall can be further thinned or higher order WGMs can be used to have a larger fraction of the resonant light inside the coated layer and therefore higher sensitivity for changes

in the stationary phase. Active thermal control will also be exploited to reduce the noise level.

While we will be working to optimize the separation of highly polar analytes such as DMMP, the presence of a tail that presents a different peak shape for this targeted analyte compared to the shapes of background chemicals may be used to our advantage. Since there generally very few analytes present in the environment at detectable levels, the separation capability does not need to be very high, enabling the use of short columns and rapid separation systems. However, the range of chemicals that could be present is large so the system must be able to discriminate target species from other analytes that may have similar retention times. For this discrimination, the characteristic tailing of DMMP (a nerve agent surrogate) could provide the added discrimination needed. Many important applications such as chemical agent or explosives detection have highly polar target analytes where this type of peak shape discrimination may be useful.

In this initial investigation, we have only focused on isothermal separations. There are several applications where the volatility range of the analytes of interest is narrow enough that isothermal separations may be sufficient, especially using short columns and rapid separations. For example, the priority nerve and blister agents have a fairly narrow range of retention times and tests with simulants indicate that they can be effectively separated on short isothermal columns. However, there are other applications where temperature programmed separations will be required to effectively separate the full range of target analytes. Since the CBORR detection is based on RI change that is affected by temperature,[21] the baseline response will change with increasing column temperature. If the temperature ramp is controlled, it may be possible to detect the sharp peaks on the moving baseline of the CBORR. Alternatively, a reference channel or temperature calibration curve may be needed to compensate for the WGM shift caused by temperature ramps.

CONCLUSIONS

We have demonstrated a rapid μGC that utilizes a capillary based optical ring resonator as an on-column detection system that is capable of separating and detecting a broad range of chemical compounds. The optical detection unit is easily adaptable to existing GC apparatus, having the advantage of small size and a circular capillary format similar to conventional GC columns. It allows for multiple on-column detection spots and optimization of each CBORR unit for different analyte detection. We have also shown the potential of the system to identify different substances by reproducible separation of several samples injected simultaneously. The advantage over many existing GC and μGC systems is its rapid response and high selectivity over a short length of active column. This μGC system shows a great potential for further development of micro gas chromatographic instruments that utilize small size and low power consumption, thus allowing for portability and field applications, and providing unique multiple on-column detection capabilities.

(21) Suter, J. D.; White, I. M.; Zhu, H.; Fan, X. *Appl. Opt.* **2007**, *46*, 389−396.